Tlapallite $H_6(Ca,Pb)_2(Cu,Zn)_3SO_4(TeO_3)_4TeO_6$ –a multi anion mineral -a Raman spectroscopic study

Ray L. Frost •

Inorganic Materials Research Program, School of Physical and Chemical Sciences, Queensland University of Technology, GPO Box 2434, Brisbane Queensland 4001, Australia.

ABSTRACT

Tellurates may be subdivided according to formula and structure. There are three types of tellurate minerals: type (a) $(AB)_m(TeO_4)_pZ_q$, type (b) $(AB)_m(TeO_6).xH_2O$ and type (c), compound tellurates in which a second anion is involved. Tlapallite, a multi anion mineral containing both tellurate and tellurite units, as well as sulphate, is an example of type (a). Tellurates are rare minerals as the tellurate ion is easily reduced to the tellurite ion. Raman bands at 691, 708, 764 and 796 cm^{-1} are attributed to $(TeO_6)^{2-}$ and $(TeO_3)^{2-}$ stretching bands. The intense sharp Raman band at 973 cm^{-1} is assigned to the ν_1 $(SO_4)^{2-}$ symmetric stretching mode, whilst the two bands at 1062 and 1104 cm^{-1} are assigned to the ν_3 $(SO_4)^{2-}$ antisymmetric stretching mode. The spectral region 100 to 600 cm^{-1} displays the bands which are attributable to the $(SO_4)^2$, $(TeO_3)^{2-}$ and $(TeO_6)^{4-}$ bending modes. Some evidence from very low intensity Raman bands in the 2800 to 3600 cm^{-1} region provides evidence of proton-tellurate/tellurite anion interactions.

*Keywords***:** Tellurate, Tellurite, Tlapallite, Raman Spectroscopy, Rodalquilarite

• Author to whom correspondence should be addressed (r.frost@qut.edu.au)
Tel. +61 7 3138 2407 Fax +61 7 3138

1. Introduction

There exists in nature, a collection of minerals based upon the elements selenium and tellurium. These minerals are the tellurates/selenates and the tellurites/selenites. They minerals may be subdivided into groups according to formula and structure [1]. There are five groups based upon the formulae (a) $A(XO_3)$, (b) $A(XO_3)\cdot xH_2O$, (c) $A_2(XO_3)_3\cdot xH_2O$, (d) $A_2(X_2O_5)$ and (e) $A(X_3O_8)$. Of the selenites, molybdomenite is an example of type (a); chalcomenite, clinochalcomenite, cobaltomenite and ahlfeldite are examples of type (b) mandarinoite is an example of type (c). There are no known examples of selenite minerals with formulae (d) and (e). The tellurite group, however, consists of minerals that can be categorised into each of the five formula types. Tellurates are very rare minerals because the tellurate anion is very easily reduced to the tellurite anion. There are three types of tellurate minerals: type (a) $(AB)_m(TeO_4)_pZ_q$, type (b) $(AB)_m(TeO_6)\cdot xH_2O$ and type (c), compound tellurates in which a second anion is involved. An example of type (a) is the mineral xocomecatlite [2-4]. Kuranakhite is also an example from this group. Xocomecatlite, $Cu_3TeO_4(OH)_4$, is related to the mineral tlalocite, $Cu_{10}Zn_6(TeO_3)(TeO_4)_2Cl(OH)_{25}\cdot 27H_2O$. Both originate from Moctezuma, Sonora, Mexico. Another related tellurate mineral is tlapallite $H_6(Ca,Pb)_2(Cu,Zn)_3SO_4(TeO_3)_4TeO_6$ which is a mixed anionic mineral containing both tellurate and tellurite anions.

In contrast to the extensive list of tellurites, there are very few tellurate minerals. The tellurate ion can be either TeO_4^{2-} or TeO_6^{6-}. Unlike sulphate, tellurate is a good oxidizing agent; it can be reduced to tellurite or tellurium. The E^0 value is significant as it gives an indication of the strength of the tellurate ion as an oxidising agent.

$$TeO_4^{2-} \rightarrow TeO_3^{2-} + 1/2O_2 \quad (E^0 = -1.042V)$$

Tellurate exists in two forms, metatellurate ion, TeO_4^{2-}, and orthotellurate ion, TeO_6^{6-}. Compounds include both metatellurates and orthotellurates. Metatellurates are analogous to sulfates, however, they are rare. Orthotellurates are much more common and therefore forms most of the chemistry of tellurates. In neutral

conditions, pentahydrogen orthotellurate ion, $H_5TeO_6^-$, is most common; in basic conditions, tetrahydrogen orthotellurate ion, $H_4TeO_6^{2-}$, is most common and in acid conditions, the orthotelluric acid, H_6TeO_6, is more common. The number of tellurate minerals is greatly overshadowed by the number of tellurites minerals, minerals containing TeO_3^{2-} units. A mineral which contains both tellurate and tellurite anions is the mineral tlapallite. The powder X-ray diffraction patterns obtained by Williams and Duggan showed that the mineral was monoclinic with a formula $H_6Ca_2Cu_3(SO_4)(TeO_3)_4TeO_6$ with a Te^{4+}/Te^{6+} ratio 4 [5].

Raman spectroscopy has proven very useful for the study of minerals [6-10]. Indeed, Raman spectroscopy has proven most useful for the study of diagenetically related minerals as tellurate and tellurite minerals often are. Some previous studies using Raman spectroscopy have been undertaken by the authors to explore the structure of minerals [11-20]. The aim of this paper is to present Raman of the natural selected mixed anion mineral tlapallite which contains both tellurate and tellurite anions and to discuss the spectra from a structural point of view. It is part of systematic studies on the vibrational spectra of minerals of secondary origin in the oxide supergene zone and their synthetic analogs.

2. Experimental

2.1 Minerals

The mineral tlapallite was sourced from Mina Bambollita, Moctezuma, Sonora, Mexico. This is the type mineral. The composition of the same mineral, obtained from different sources, has been reported by Anthony *et al.* (page 709) [21].

2.2 Raman microprobe spectroscopy

Crystals of the tlapallite mineral were placed and orientated on the stage of an Olympus BHSM microscope which was equipped with 10x and 50x objectives as part of a Renishaw 1000 Raman microscope system. The system also includes a monochromator, filter system and Charge Coupled Device (CCD). Raman spectra

were excited by a HeNe laser (633 nm) at a resolution of 2 cm^{-1} in the range between 100 and 4000 cm^{-1}. Repeated acquisition using the highest magnification was accumulated to improve the signal to noise ratio. Spectra were calibrated using the 520.5 cm^{-1} line of a silicon wafer.

Spectroscopic manipulation such as baseline adjustment, smoothing and normalisation were performed using the Spectracalc software package GRAMS (Galactic Industries Corporation, NH, USA). Band component analysis was undertaken using the Jandel 'Peakfit' software package, which enabled the type of fitting function to be selected and allows specific parameters to be fixed or varied accordingly. Band fitting was done using a Gauss-Lorentz, cross-product function with the minimum number of component bands used for the fitting process. The Gauss-Lorentz ratio was maintained at values greater than 0.7 and fitting was undertaken until reproducible results were obtained with squared correlations (r^2) greater than 0.995.

3. Results and discussion

Farmer [22] states that very little research has been undertaken on the vibrational spectroscopy of tellurates. As such very few papers have been forthcoming. Only a few minerals with the tellurate anion have been discovered [2-4]. The metatellurate anion TeO_4^{2-} should have T_d symmetry and therefore four internal modes, namely A_1 (ν_1), E (ν_2) and $2F_2$ (ν_3 and ν_4) . The orthotellurate ion, TeO_6^{6-} will have octahedral symmetry but may be strongly distorted. Vibrational modes for the tellurate anion should occur in the 620 to 650 cm^{-1} region and in the 290 to 360 cm^{-1} region. If the symmetry of the tellurate anion is reduced through for example bonding to a cation as in the kuranakhite structure then the loss of degeneracy will occur, and additional bands observed. Siebert [23] reported the infrared spectra of selected synthetic tellurates and antimonates. The position of the bands for the TeO_6^{6-} anion was defined by Siebert as ν_1 650 cm^{-1} (A_{1g}), ν_3 630 cm^{-1} (E_g), ν_2 375 cm^{-1} (F_{2g}). For the compound H_6TeO_6 infrared bands were observed at 605, 650, 658, 675, 708 and 730 cm^{-1} and were assigned to TeO stretching vibrations. In addition an intense band at 411 cm^{-1} is assigned to a δTeO bending mode

(presumably ν_4 vibration). For the compound $Na_2H_4TeO_6$ infrared bands were observed at 429, 536, 587, 675 and 780 cm^{-1}. More complexity was observed in the spectrum of $K_2H_4TeO_6 \cdot 3H_2O$. Siebert also provided data for the compound $(H_4TeO_4)_x$. For this polytellurous acid, infrared bands were found at 450 cm^{-1} (δTeO) and stretching modes at 600, 720, 800 cm^{-1}. According to Siebert the TeO_6^{6-} anion is octahedral but is distorted. Thus infrared forbidden bands are activated.

The Raman spectrum of tlapallite in the 600 to 900 cm^{-1} region is shown in Figure 1. The spectral profile displays Raman bands at 764 and 796 cm^{-1}, Raman bands are observed also at 691 and 708 cm^{-1}. It is difficult to nominate a specific cause for each of these bands but one possible suggestion is as follows: the higher wavenumber bands may be attributed to the tellurate ion $(TeO_6)^{2-}$ and the lower wavenumber bands to the tellurite anion $(TeO_3)^{2-}$. Thus, the Raman band at 796 cm^{-1} is attributed to the ν_1 $(TeO_6)^{2-}$ symmetric stretching mode and the band at 764 cm^{-1} to the ν_1 $(TeO_3)^{2-}$ symmetric stretching mode. The band at 708 cm^{-1} may be attributed to the ν_3 $(TeO_6)^{2-}$ antisymmetric stretching mode and the band at 691 cm^{-1} to the ν_1 $(TeO_3)^{2-}$ antisymmetric stretching mode. The Raman spectrum in the 900 to 1700 cm^{-1} region is shown in Figure 2. This spectral region is where the $(SO_4)^{2-}$ stretching bands may be observed. The intense, sharp Raman band at 973 cm^{-1} is assigned to the ν_1 $(SO_4)^{2-}$ symmetric stretching mode, whilst the two bands at 1062 and 1104 cm^{-1} are assigned to the ν_3 $(SO_4)^{2-}$ antisymmetric stretching mode. The low intensity Raman bands at 1474 and 1571 cm^{-1} may be associated with the protons via formation of OH units. Alternatively, the bands may be associated with bands, associated with amorphous carbon. Such bands may originate from handling of the sample and the burning of organic residues by the incident laser.

A comparison may be made with the Raman spectra of other tellurate minerals. In the Raman spectrum of xocomecatlite $Cu_3(OH)_4TeO_4 \cdot H_2O$ a broad band that may be decomposed into component bands at 710, 763 and 796 cm^{-1}. Thee bands are quite sharp. One possible assignment is the band at 796 cm^{-1} is ascribed to the TeO_4 ν_1 symmetric stretching mode and the two bands at 710 and 763 cm^{-1} to the TeO_4 antisymmetric stretching mode. Two bands for of kuranakhite $PbMn^{4+}Te^{6+}O_6$ observed at 617 and 686 cm^{-1} are assigned to the $Te^{6+}O_6$ ν_1 symmetric stretching

mode. The observation of two bands suggests the non equivalence of the $Te^{6+}O_6$ in the structure. Such a concept would need to be confirmed by X-ray diffraction. The broad band centred at 743 cm^{-1} is attributed to the $Te^{6+}O_6$ ν_3 antisymmetric stretching mode. The width of this band may indicate that it is composed of a number of overlapping bands. The assignment of the $Te^{6+}O_6$ stretching bands is at variance to that proposed by Siebert. [23]

In terms of tellurite anion a comparison may be made with the Raman spectra of other tellurite minerals. For example, two Raman bands for rajite observed at 754 and 731 cm^{-1} are assigned to the ν_1 $(Te_2O_5)^{2-}$ symmetric stretching mode. The two bands at 652 and 603 cm^{-1} are assigned to the ν_3 $(Te_2O_5)^{2-}$ antisymmetric stretching mode. An intense band observed at 734 cm^{-1} for denningite, is attributed to the ν_1 $(Te_2O_5)^{2-}$ symmetric stretching mode. The Raman band of denningite, at 674 cm^{-1}, is assigned to the ν_3 $(Te_2O_5)^{2-}$ antisymmetric stretching mode. Two Raman bands for zemannite are observed at 745 and 647 cm^{-1}. These bands are assigned to the ν_1 $(TeO_3)^{2-}$ symmetric stretching mode and the ν_3 $(TeO_3)^{2-}$ antisymmetric stretching mode, respectively. Two Raman bands, observed at 763 and 791 cm^{-1} for emmonsite, are assigned to the ν_1 $(TeO_3)^{2-}$ symmetric stretching mode whilst the Raman bands displayed at 679 and 567 cm^{-1} are assigned to the ν_3 $(TeO_3)^{2-}$ antisymmetric stretching mode.

The low wavenumber region of tlapallite, 100 to 600 cm^{-1}, is shown in Figure 3. This region displays those bands which are attributable to the $(SO_4)^{2-}$, $(TeO_3)^{2-}$ and $(TeO_6)^{4-}$ bending modes. The complexity of the spectrum makes assignment difficult. One possible set of assignments is as follows: the band at 610 cm^{-1} (Figure 1) may be assigned to the $(SO_4)^{2-}$ ν_4 bending mode and the intense band at 438 cm^{-1} may be attributed to the $(SO_4)^{2-}$ ν_2 bending mode. The two Raman bands of tlapallite, at 314 and 353 cm^{-1}, may be assigned to the $(TeO_3)^{2-}$ ν_2 (A_1) bending mode and the two bands, at 383 and 419 cm^{-1}, may be assigned to the $(TeO_3)^{2-}$ ν_4 (E) bending mode. The remaining bands, at 474 and 509 cm^{-1}, may be assigned to the $(TeO_6)^{4-}$ ν_4 and ν_2 bending modes. The Raman bands at 229, 258 and 291 cm^{-1} may be associated with MO and OMO stretching and bending vibrations where M may be Cu, Zn, Ca or Pb.

Raman bands for rajite, observed at (346, 370) and 438 cm^{-1} are assigned to the $(Te_2O_5)^{2-}$ ν_2 (A_1) bending mode and ν_4 (E) bending mode. The very weak Raman bands of denningite at 450 and 479 cm^{-1} are assigned to the $(Te_2O_5)^{2-}$ ν_4 (E) bending modes and the bands at 349 and 381 cm^{-1} are assigned to the $(Te_2O_5)^{2-}$ ν_2 (A_1) bending mode. Raman bands are observed at 372 and 408 cm^{-1} for zemmanite and 397 and 414 cm^{-1} for emmonsite, both of which may be due to the $(TeO_3)^{2-}$ ν_2 (A_1) bending mode. Two low intensity bands in the Raman spectrum of graemite, at 314 and 358 cm^{-1}, may be assigned to the $(TeO_3)^{2-}$ ν_2 (A_1) bending mode. The intense bands at 411, 438 and 471 cm^{-1} may be assigned to the $(TeO_3)^{2-}$ ν_4 (E) bending mode. The sharp Raman band for teineite at 235 cm^{-1} may be attributed to CuO stretching vibrations. The two sharp bands for graemite at 257 and 291 cm^{-1} may also be attributed to CuO stretching vibrations.

The Raman spectrum of tlapallite in the 1800 to 3200 cm^{-1} region is displayed in Figure 4. The spectrum suffers from a low of signal to noise ratio. This is not unexpected as there are no water or OH units in the tlapallite structure. The scale of the spectrum has been increased. Bands in this spectral region may result from induced OH units formed by the interaction of the protons with the sulphate, tellurite or tellurate units. Bands are identified at around 1957, 2206, 2326, 2594, 2754, 2867 and 2926 cm^{-1}. These bands are attributed to OH stretching vibrations formed by the interaction of the protons with the oxygen of the tellurate/tellurite units. Alternatively some of these very low intensity bands may well be identifying surface contamination by organic molecules, perhaps through handling. The bands in the 2850 to 2950 cm^{-1} may well be assigned to CH stretching vibrations.

Studies have shown a strong correlation between OH stretching frequencies and both O···O bond distances and H···O, hydrogen bond distances [24-27]. Libowitzky (1999) showed that a regression function can be employed relating the hydroxyl stretching frequencies with regression coefficients better than 0.96 using infrared spectroscopy [28]. The function is described as: $\nu_1 = (3592 - 304) \times 109^{\frac{-d(O-O)}{0.1321}}$ cm^{-1}. Thus, OH···O, hydrogen bond distances may be calculated using the Libowitzky empirical function. The values for the OH stretching

vibrations listed above provide hydrogen bond distances of 2.537(0) Å (2206 cm^{-1}), 2.549(3) Å (2326 cm^{-1}), 2.580(7) Å (2594 cm^{-1}), 2.603(5) Å (2754 cm^{-1}), 2.622(7) Å (2867 cm^{-1}) and 2.633(9) Å (2926 cm^{-1}) which are very short compared with that of many secondary minerals. Normally, large hydrogen bond distances, which are present in minerals such as perhamite, can also be seen in other mixed anion minerals, such as peisleyite, where the distances range between 3.052(5) and 2.683(6) Å. Such hydrogen bond distances are typical of secondary minerals. A range of hydrogen bond distances are observed from reasonably strong to weak hydrogen bonding. This range of hydrogen bonding contributes to the stability of the mineral. In the case of tlapallite, the proton-tellurite interactions contribute to the stability of this tellurite mineral to compensate for the lack of stability provided by the larger hydrogen bond distances.

4. Conclusions

In nature, very few tellurate minerals exist. They may be subdivided according to formula and structure. The tellurate ion is TeO_4^{2-} or TeO_6^{6-}. Unlike sulfate, tellurate is a good oxidizing agent; it can be reduced to tellurite or even tellurium metal. As a result of this, the quantity of tellurite minerals greatly out numbers the quantity of tellurate minerals. The ready reduction of the tellurate anion to the tellurite anion leads to certain minerals such as tlapallite forming mixed anionic species in which both the tellurate and tellurite ions exist.

The Raman spectrum of the mixed anion tellurate mineral tlapallite, has been studied using Raman spectroscopy. Observed bands were tentatively assigned to the stretching and bending vibrations of the tellurite anion, $(TeO_3)^{2-}$, the tellurate anion and sulphate anion. Because of the potential overlap of bands ascribed to the tellurate and tellurite anions, assignment of bands is not simple. It is difficult to nominate a specific cause for each of these bands but one possible suggestion is as follows: the higher wavenumber bands may be assigned to the tellurate anion, $(TeO_6)^{2-}$, and the lower wavenumber bands to the tellurite anion, $(TeO_3)^{2-}$. Thus, the Raman band at 796 cm^{-1} may be assigned to the ν_1 $(TeO_6)^{2-}$ symmetric stretching mode and the band at 764 cm^{-1} to the ν_1 $(TeO_3)^{2-}$ symmetric stretching mode. The band at 708 cm^{-1} may

be assigned to the ν_3 $(TeO_6)^{2-}$ antisymmetric stretching mode and the band at 691 cm^{-1} to the ν_1 $(TeO_3)^{2-}$ antisymmetric stretching mode. The band at 610 cm^{-1} may be assigned to the $(SO_4)^{2-}$ ν_4 bending mode. The intense band at 438 cm^{-1} may be attributed to the to the $(SO_4)^{2-}$ ν_2 bending mode. The two Raman bands of tlapallite at 314 and 353 cm^{-1} may be assigned to the $(TeO_3)^{2-}$ ν_2 (A_1) bending mode and the two bands for teineite at 383 and 419 cm^{-1} may be assigned to the $(TeO_3)^{2-}$ ν_4 (E) bending mode. The remaining bands at 474 and 509 cm^{-1} may be assigned to the $(TeO_6)^{4-}$ ν_4 and ν_2 bending modes.

Acknowledgements

The financial and infra-structure support of the Queensland University of Technology Inorganic Materials Research Program of the School of Physical and Chemical Sciences is gratefully acknowledged. The Australian Research Council (ARC) is thanked for funding the instrumentation.

REFERENCES

[1] J.D. Dana, Dana's Manual of Mineralogy, by W. E. Ford. 22nd edition, Wiley London 2006

[2] A.C. Roberts, J.D. Grice, L.A. Groat, A.J. Criddle, R.A. Gault, R.C. Erd, E.A. Moffatt, Can. Min.34 (1996) 49-54.

[3] A.C. Roberts, T.S. Ercit, A.J. Criddle, G.C. Jones, R.S. Williams, F.F. Cureton, II, M.C. Jensen, Min. Mag. 58 (1994) 417-424.

[4] S.A. Williams, Min. Mag. 40 (1975) 221-226.

[5] S.A. Williams, M. Duggan, Min. Mag. 42 (1978) 183-186.

[6] R.L. Frost, J. Cejka, G.A. Ayoko, M.J. Dickfos, J. Raman Spectrosc. 39 (2008) 374-379.

[7] R.L. Frost, M.J. Dickfos, J. Cejka, J. Raman Spectrosc. 39 (2008) 582-586.

[8] R.L. Frost, M.C. Hales, D.L. Wain, J. Raman Spectrosc. 39 (2008) 108-114.

[9] R.L. Frost, E.C. Keeffe, J. Raman Spectrosc. in press (2008).

[10] S.J. Palmer, R.L. Frost, G. Ayoko, T. Nguyen, J. Raman Spectrosc. 39 (2008) 395-401.

[11] R.L. Frost, J.M. Bouzaid, J. Raman Spectrosc. 38 (2007) 873-879.

[12] R.L. Frost, J.M. Bouzaid, W.N. Martens, B.J. Reddy, J. Raman Spectrosc. 38 (2007) 135-141.

[13] R.L. Frost, J. Cejka, J. Raman Spectrosc. 38 (2007) 1488-1493.

[14] R.L. Frost, J. Cejka, G.A. Ayoko, M.L. Weier, J. Raman Spectrosc. 38 (2007) 1311-1319.

[15] R.L. Frost, J. Cejka, M.L. Weier, J. Raman Spectrosc. 38 (2007) 460-466.

[16] R.L. Frost, J. Cejka, M.L. Weier, W.N. Martens, G.A. Ayoko, J. Raman Spectrosc. 38 (2007) 398-409.

[17] R.L. Frost, M.J. Dickfos, J. Raman Spectrosc. 38 (2007) 1516-1522.

[18] R.L. Frost, S.J. Palmer, J.M. Bouzaid, B.J. Reddy, J. Raman Spectrosc. 38 (2007) 68-77.

[19] R.L. Frost, C. Pinto, J. Raman Spectrosc. 38 (2007) 841-845.

[20] R.L. Frost, M.L. Weier, P.A. Williams, P. Leverett, J.T. Kloprogge, J. Raman Spectrosc. 38 (2007) 574-583.

[21] J.W. Anthony, R.A. Bideaux, K.W. Bladh, M.C. Nichols, Handbook of Mineralogy, Mineral Data Publishing, Tuscon, Arizona, USA, 2000.

[22] V.C. Farmer, Editor, Mineralogical Society Monograph 4: The Infrared Spectra of Minerals, 1974.

[23] H. Siebert, Z. anorg. u. allgem. Chem. 301 (1959) 161-170.

[24] J. Emsley, Chem. Soc. Rev. 9 (1980) 91-124.

[25] H. Lutz, Struct. Bond. 82 (1995) 85-103.

[26] W. Mikenda, J. Mol. Struct. 147 (1986) 1-15.

[27] A. Novak, Struct. Bond. 18 (1974) 177-216.

[28] E. Libowitsky, Monats. Chem. 130 (1999) 1047-1049.

List of Figures

Figure 1 Raman spectrum of tlapallite in the 600 to 900 cm^{-1} region

Figure 2 Raman spectrum of tlappalite in the 900 to 1700 cm^{-1} region

Figure 3 Raman spectrum of tlappalite in the 100 to 600 cm^{-1} region

Figure 4 Raman spectrum of tlappalite in the 1800 to 3200 cm^{-1} region

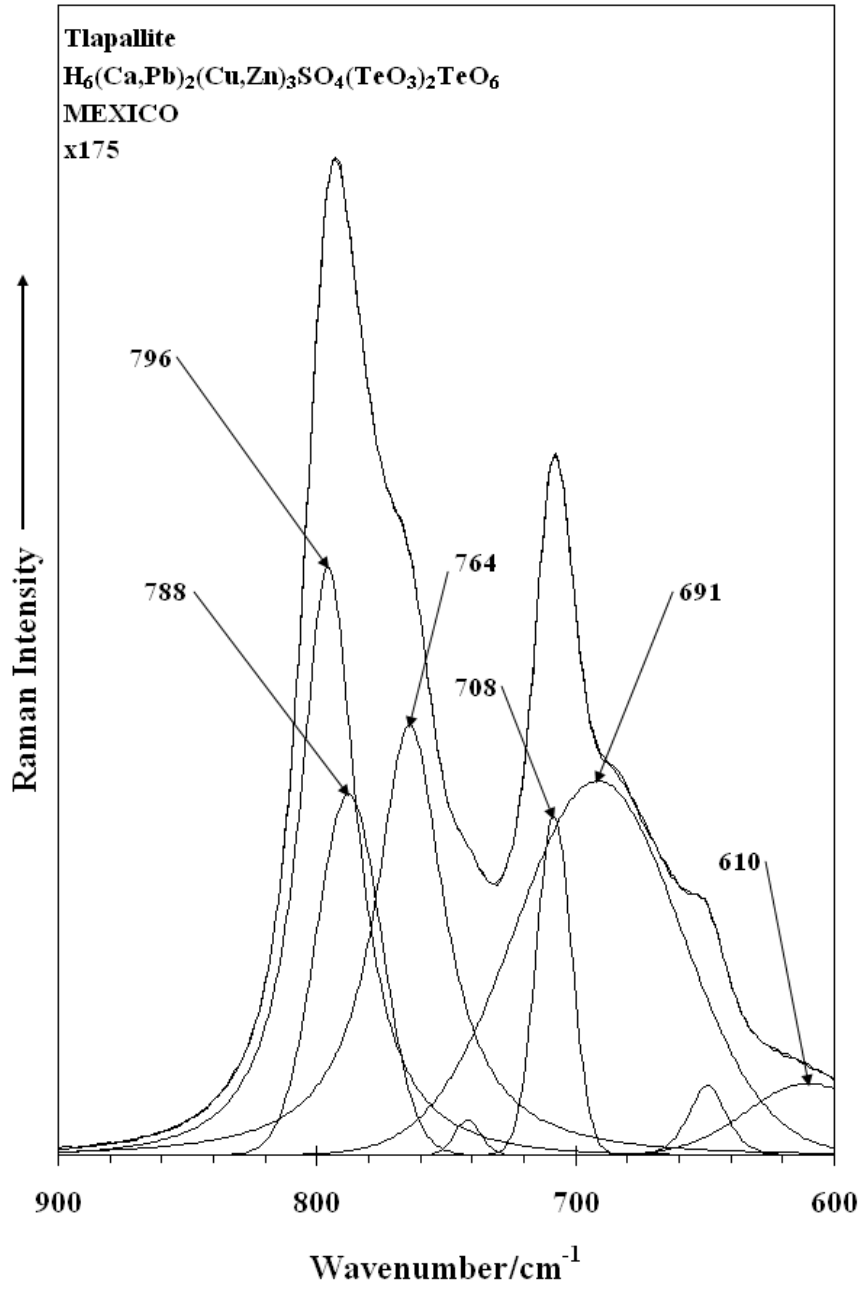

342
343
344 **Figure 1 tlapallite**
345
346

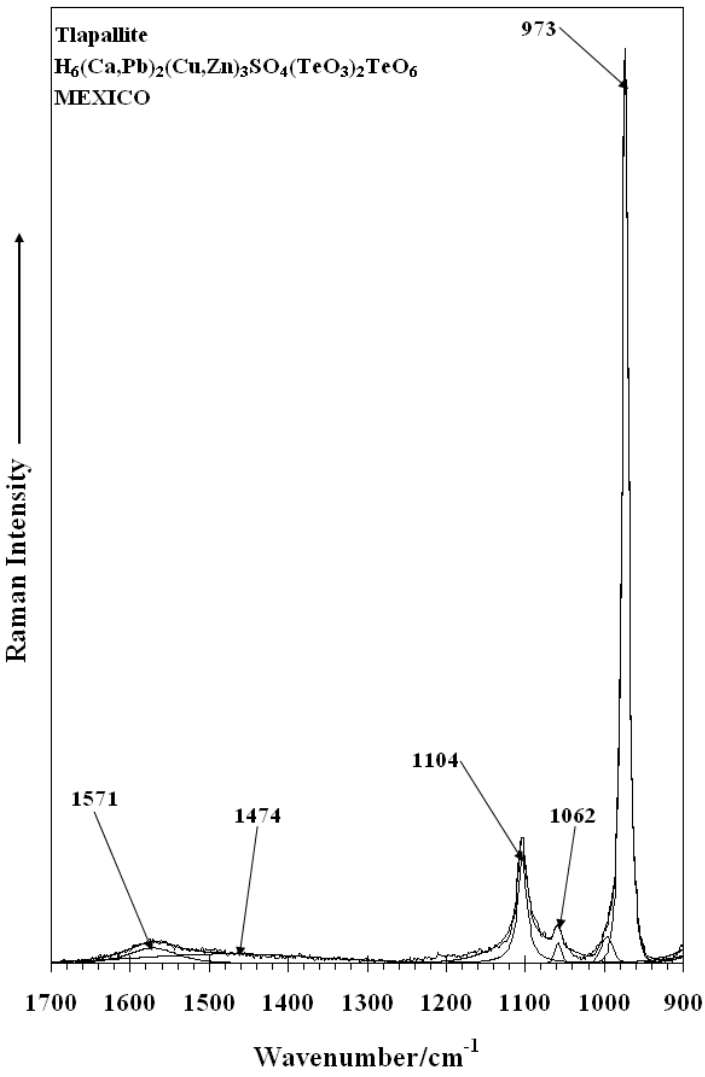

347

348

349 **Figure 2**

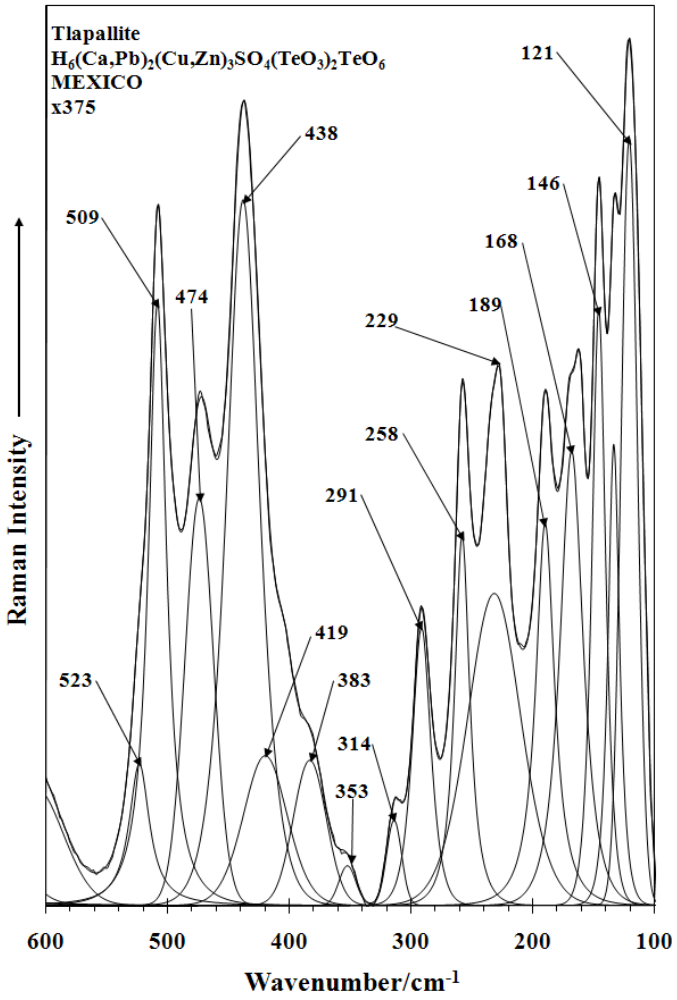

Figure 3 tlapallite

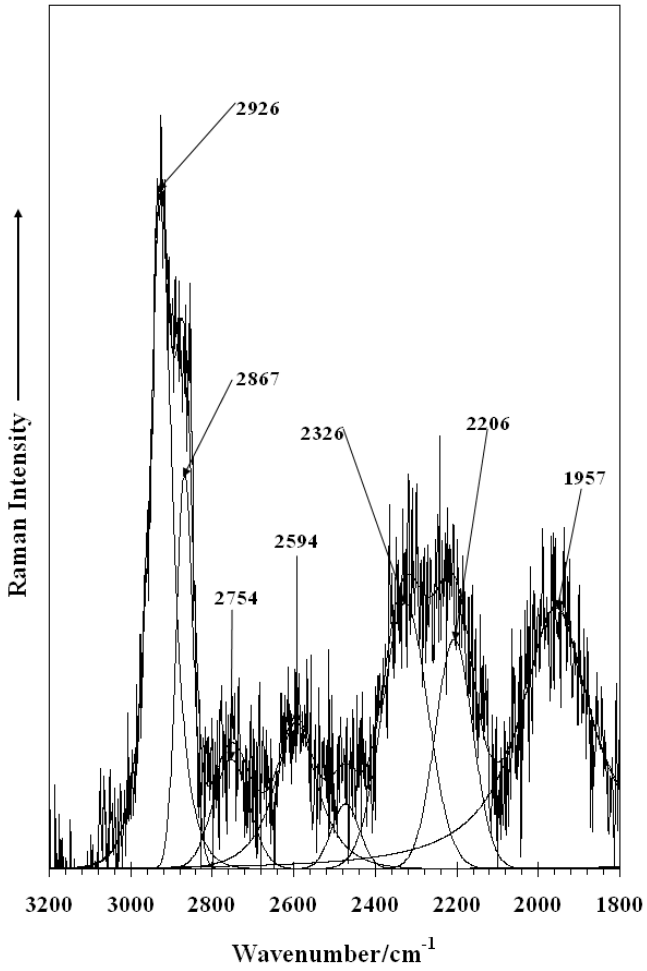

355

356

357 **Figure 4**

358

359